

Expanded Poster-Prize Abstracts

SAXS study of the influence of added clay particles on a block copolymer gel

V. Castelletto & I. W. Hamley

Department of Chemistry, University of Leeds, Leeds, LS2 9JT, UK

Received 28th October 2003; accepted in revised form 16th March 2004

1. Introduction

Inorganic filler particles are added to soft materials such as polymers to improve their mechanical properties, and also to alter properties such as colour, flame resistance or permeability. Clay particles are plate-like mineral moieties, based on silicates or aluminosilicates [1]. They are widely used in those applications due to their ease of availability and processing and low cost. A recent focus has been on polymer-clay nanocomposites, in which the polymer chains are intercalated between clay layers [2].

In the present study, we investigate the effect of added clay particles on the structural and rheological properties of a hexagonal (H) mesophase formed by a triblock copolymer surfactant. An account of this work has been published recently [3]. However, some details of the calculation of the lamellar elasticity from the structure factor were incorrect, as discussed herein. The clay particles used are the synthetic hectorite, Laponite RDS. The triblock employed here is one of the widely used Pluronic family of poly(oxyethylene)-poly(oxypropylene)-poly(oxyethylene) (EPE) polymer surfactants - P123 ($E_{20}P_{70}E_{20}$). We are not aware of previous studies of the structure or rheology of Laponite RDS suspensions. Laponite RDS differs from the more widely used Laponite RD due to the presence of a peptizing agent. The influence of shear on the orientation of PEO chains and Laponite RDS particles has been studied by SANS on mixtures of these two components in aqueous solution [4]. There has been also limited prior work on mixed Laponite/surfactant solutions. The adsorption of non-ionic surfactants ($C_{12}E_5$ and $C_{12}E_8$, C=methyl) onto Laponite RD particles has been investigated by adsorption isotherm and small-angle neutron scattering measurements (SANS) [5]. In a subsequent study, the location of Laponite particles in the swollen lamellar (L) or sponge phase of aqueous solutions of $C_{12}E_5$ and $C_{12}E_4$ was probed by SANS [6].

2. Experimental Section

2.1. Materials. The synthetic clay used was Laponite RDS, obtained as a gift from Rockwood Additives Ltd. Laponite RDS particles are stable at pH 9.5, so our solutions are prepared under these alkaline conditions [7-11]. Block copolymer surfactant Pluronic P123 was obtained as a gift from Uniqema. The molecular weight of this triblock copolymer is 5750 g mol⁻¹ [12]. The phase diagram of P123 in water has been reported [13].

2.2. Preparation of Mixtures. The clay dispersions were prepared by slowly adding Laponite RDS powder to ultrapure water (Milli-Q-Plus) with constant stirring for at least 15 min. The pH of the dispersions was maintained at 9.5 by adding analytical grade NaOH. Mixtures were prepared by adding aqueous gels containing Pluronic surfactant to Laponite solutions of different concentrations, such that the final mass fraction of P123 defined as $w_S = m(\text{P123}) / [m(\text{P123}) + m(\text{Laponite} + \text{water})]$ was $w_S = 0.5$ (50wt%), where m denotes mass. The mass fractions of Laponite are defined as $w_L = m(\text{Laponite}) / [m(\text{Laponite}) + m(\text{water})]$ [6].

2.3. Small angle X-ray Scattering (SAXS). SAXS experiments were performed at the Synchrotron Radiation Source (SRS) at Daresbury Laboratory, Warrington, UK. Samples were studied either at rest or after oscillatory shear. Static experiments were performed on beamlines 8.2 and 2.1, while shear flow experiments were undertaken on beamline 16.1. All three stations are configured with an X-ray wavelength $\lambda = 1.5$ Å. On station 8.2 the scattered intensity was recorded using a quadrant SAXS detector that measures intensity in the radial direction, while on both beamline 2.1 and station 16.1, the scattered intensity was recorded on a multiwire gas-filled area detector. A scattering pattern from a specimen of wet collagen (rat-tail tendon) was used for calibration of the q scale ($q = |\mathbf{q}| = (4\pi \sin \theta) / \lambda$, where the scattering angle is 2θ) of the scattering profile.

For the static measurements the samples were mounted in sealed 1 mm thick brass cells, with an inner spacer ring to hold liquids, sealed between mica windows, and connected to a water bath for temperature control. Oscillatory shear was applied to the samples using a Rheometrics RSA II soft solids system with shear sandwich geometry. A detailed description of the rheometer is provided elsewhere [14,15]. It enables simultaneous acquisition of SAXS and rheology data. The shear sandwich cell comprises three rectangular plates, perpendicular to the X-ray beam, which is incident along ∇v , so that the $(\mathbf{q}_v, \mathbf{q}_e)$ plane is accessed in SAXS experiments.

3. Results and Discussion

Laponite particles have previously been shown to be plate-like. The SAXS data for 2 wt % Laponite RDS in aqueous solution at pH 10 was fitted to the form factor corresponding to a disk-like particle with thickness Γ and radius R [16] (Figure 1). The fitting provided $2R = (35.3 \pm 0.3)$ nm and $\Gamma = (2.1 \pm 0.1)$ nm. The

values $2R = 30$ nm, $\Gamma = 1$ nm and $2R = 25$ nm, $\Gamma = 0.9$ nm were reported, for Laponite RD, by Mourchid [7] and Kroon [17] respectively. Compared to the previous results for Laponite RD, the diameter and thickness reported here for Laponite RDS are both increased due presumably to the adsorbed anions.

The structure of gels containing 0-9 wt % added Laponite RDS at pH 10 was determined by SAXS, in the temperature range from 25 to 75 °C. The main feature of the SAXS patterns for gels of P123 in the absence of Laponite, is a series of Bragg reflections located in the positional ratio 1: $\sqrt{3}$: $\sqrt{4}$: $\sqrt{7}$: $\sqrt{9}$, as expected for a hexagonal lattice. These results are consistent with the previously reported phase diagram of P123 in water [13].

The SAXS intensity as a function of the temperature was then recorded for P123 gels with 3-7 wt% Laponite RDS. A discontinuity in the position of a higher order reflection, and in the intensity of the first order reflection is apparent at high temperature. We measured the position of the scattering peaks from each SAXS profile, and the results are contained in Figure 2, which shows the position of the scattering peaks as a function of temperature.

Figure 2 shows that at low temperature the gels are characterized by three to five reflections with a positional ratio 1: $\sqrt{3}$: $\sqrt{4}$: $\sqrt{7}$: $\sqrt{9}$ corresponding to the first five orders of reflection from a H structure [18]. In contrast, at high temperature only two or three reflections were measured with a positional ratio 1:2:3 within the experimental error, which are indexed to the 100, 200 and 300 reflections respectively of a L phase [18]. For intermediate temperatures, and for samples containing between 3 and 7 wt % added Laponite, a set of reflections in the positional ratio 1: $\sqrt{3}$: $\sqrt{4}$: $\sqrt{7}$ is also present, suggesting that both H and L orders co-exist in the system (Figure 2). A transition from H to L structures is not observed for a 50 wt % gel of the copolymer alone between 25 and 75 °C [13]. Therefore, the results shown in Figure 2 suggest that the addition of Laponite RDS to the system induces an H to L phase transition at high temperature.

To confirm a structural transition, SAXS patterns were obtained from samples aligned using large-amplitude oscillatory shear (frequency $\omega = 100$ rad s⁻¹ and strain amplitude $A = 70\%$). Figure 3 shows the two-dimensional SAXS patterns obtained at rest following shear, for a gel with 9 wt % Laponite RDS, at 30°C (Figure 3a) and 60°C (Figure 3b). In both cases, two pairs of equatorial reflections are observed. At 30°C, these are in the positional ratio 1: $\sqrt{3}$ and at 60°C they are in the ratio 1: 2. The former is consistent with a shear-aligned H phase in which the cylinder axis is parallel to the direction of flow, while the latter results indicate that oscillatory shear orients the layers in the L phase perpendicular to the (\mathbf{q}_v , \mathbf{q}_e) plane, with the lamellae normal parallel to the neutral axis.

From the location of the SAXS peaks it is possible to determine the domain spacing in the H and L phases as a function of temperature. In particular, the average distance between cylinders in the H phase, $d = 2\pi/q^*$ (q^* = position of the first scattering peak), is calculated in the same way as the interlayer distance d in the L phase. Figure 2 shows that q^* decreases (i.e. d increases) with temperature, and there are no discontinuities across the phase transition boundary. The fact that q^* changes

continuously across the transition (Figure 2) indicates that the transition between H and L structures is epitaxial.

It is possible to undertake a qualitative analysis of the order of the anisotropic particles dispersed in the L phase. Two relevant distances can be distinguished: the centre-to-centre particle separation, D_{2D} , and the intermembrane separation distance, D . The two-dimensional particle-particle separation, for particles located on average in the mid-plane between the surfactant lamellae separated by a water thickness D , is given by

$$D_{2D} = \sqrt{\frac{2V_L(C_L + \rho_L)}{3DC_L}}$$

(V_L : volume of a Laponite disk, C_L : mass of dried Laponite divided by the mass of water and $\rho_L = 2.53$ is the density of Laponite with respect to water). Using the parameters from the form factor fit to the SAXS profile from a Laponite disk (Figure 1), $V_L = \pi R^2 H = 1923.3$ nm³. The intermembrane separation distance $D = d(1-\phi)$ is expressed as a function of the hydrophobic layer thickness, where the d values are taken from q^* , and

$$\phi = \frac{w_s \rho_L (1 + C_L)}{d_s \rho_L + \rho_L w_s (1 - d_s) + C_L (\rho_s + w_s (\rho_L - \rho_s))}$$

is the volume fraction of polymer in the P123/Laponite/water system ($w_s = 0.5$: mass fraction of surfactant in the sample and $\rho_s = 1.05$ is the density of P123 relative to water) [12].

Figure 4 shows the evolution of D_{2D} and the fraction D_{2D}/D as a function of temperature, for different concentrations of Laponite RDS, within the L phase. As expected, the average distance between the clay disks decreases with increasing Laponite concentration (Figure 4a) as does the ratio D_{2D}/D (Figure 4b). Figures 4b-d show that the centre-to-centre distance is always higher than the intermembrane distance, ensuring enough space for the disks to freely spread between the lamellae.

These calculations on the separation of Laponite particles within and between layers confirm that there is ample space for them to be intercalated between lamellae. It is thus proposed that the H-to-L transition is driven by the increase in packing entropy of the disks in the L phase, compared to the H phase. Assuming that the particles are preferentially located in the aqueous region, the volume available to the particles is smaller in the H phase since the packing fraction of surfactant is higher. The concentration dependence of the transition arises because the excluded volume available to the particles (more of which is "explored" by the Brownian motion of particles at high temperature) decreases with increasing particle concentration.

To obtain an insight into the effect of the Laponite on the elasticity of the layers in the L phase, we used the model of Caillé [19] to fit the shape of the SAXS reflections. For aligned one-dimensional systems the scattered intensity should exhibit an asymptotic power-law behaviour $S(q) \sim |q - q_{0,m}|^{-2+\eta_m}$, where η_m is the mth- order Caillé parameter and $q_{0,m}$ is the position of the mth- order scattering peak [19,20]. This was the expression

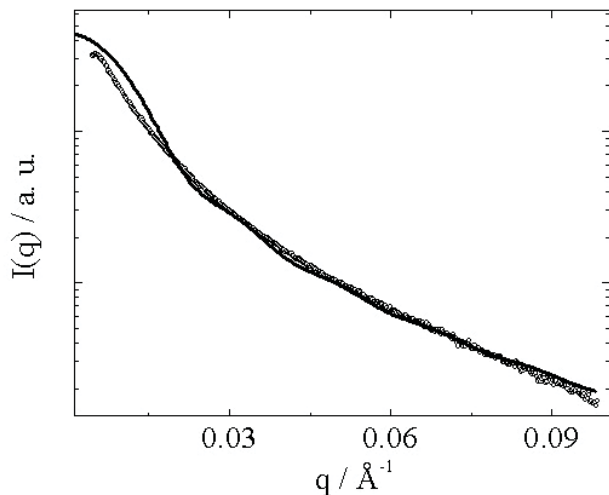


Figure 1. SAXS profile measured for a 2 wt % laponite RDS aqueous solution (O) and the calculated form factor for an isolated disk-shaped particle (—). In the model, the particle diameter and thickness are $2R = 350 \text{ \AA}$ and $\Gamma = 20 \text{ \AA}$ respectively.

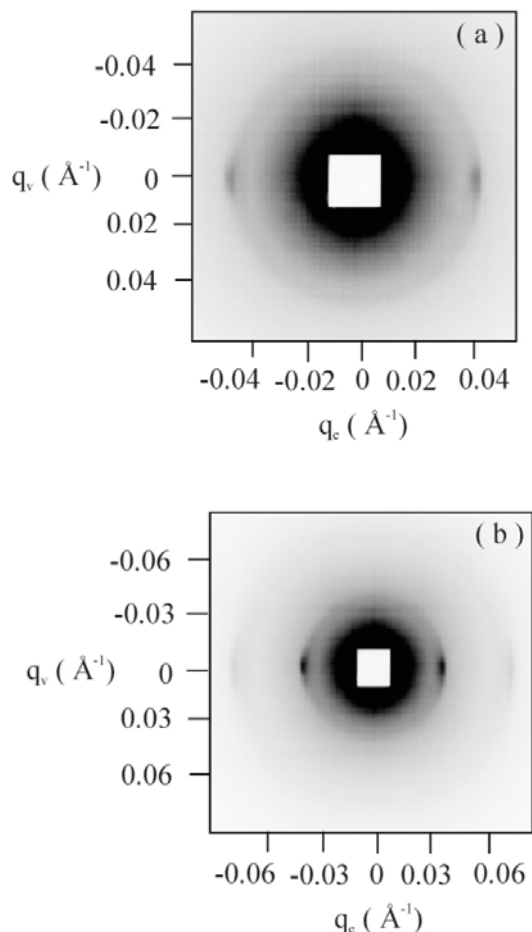


Figure 3. SAXS pattern in the (q_v, q_c) plane obtained at (a) 30°C (the second order peak is not shown in the figure because the contrast scale used does not allow first and second order reflections to be shown simultaneously) and (b) 60°C for a gel containing 9 wt% added Laponite RDS, at rest after oscillatory shear in the shear sandwich at a frequency $\omega = 100 \text{ s}^{-1}$, and strain amplitude $A = 70\%$.

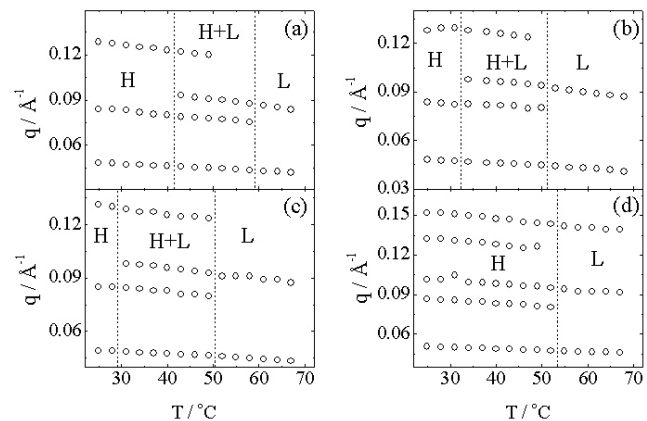


Figure 2. Temperature dependence of the Bragg peak positions for 50 wt% P123 with (a) 3, (b) 4.5, (c) 7 and (d) 9 wt% Laponite RDS. The traced lines divide the regions of hexagonal (H), lamellar (L) and H/L phase co-existence.

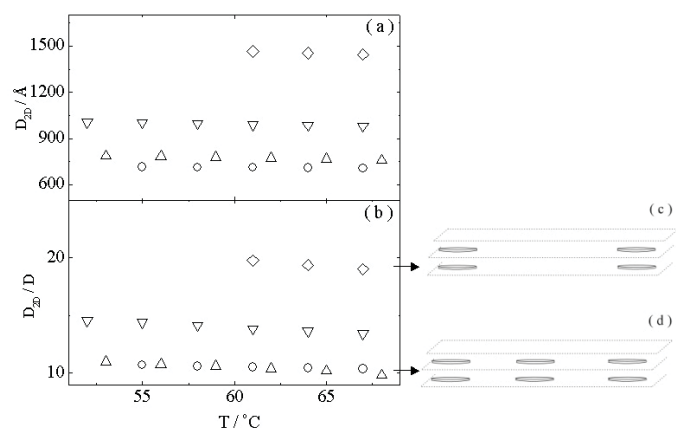


Figure 4. Dependence of (a) D_{2D} and (b) D_{2D}/D on temperature for a 50 wt % P123 gel with (\diamond) 3, (∇) 4.5, (Δ) 7 and (O) 9 wt% added Laponite RDS. Shown alongside are sketches indicating the size and spacing of disks compared to the lamellar spacing, for (c) 3 wt % added Laponite at 75°C and (d) 9 wt % added Laponite at 67°C .

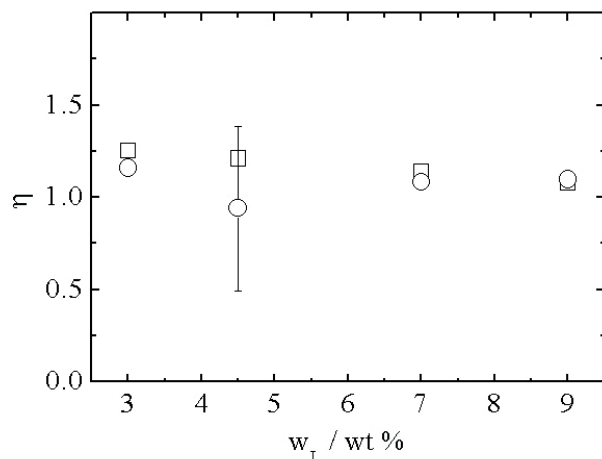


Figure 5. Dependence of the Caillé parameter on concentration of added Laponite. (O) Caillé parameter extracted from fitting peaks in the SAXS profiles, (∇) calculated according to the Helfrich model. The standard deviation of the fitted Caillé parameter is shown for 4.5 wt % added Laponite.

used previously by us [3]. However, for unoriented samples, as investigated here, we need to take a powder average. This leads to $S(q) \sim |q - q_{o,m}|^{-1+\eta_m}$ [21, 22].

An averaged value of the Caillé parameter, $\bar{\eta}$, was obtained using the set of η_m values for a particular SAXS profile, i.e. calculating the average of

$$\eta = \frac{\eta_m}{m^2} = \frac{q_o^2 k_B T}{8\pi \sqrt{KB}}$$

Here K and B are elastic and compression moduli for lamellae respectively [19,20]. The dependence of $\bar{\eta}$ on concentration of added Laponite (at a constant temperature $T = 61^\circ\text{C}$) is illustrated in Figure 5, together with the Caillé parameter calculated based on the theory of Helfrich developed for the L phase of nonionic surfactants [23]. In this model [20]

$$\eta = \frac{4}{3} \left(1 - \frac{\delta}{d}\right)^2$$

Figure 5 shows that the experimental η is very close that predicted by the Helfrich model, indicating the entropic interactions between fluctuating lamellae govern the elasticity of the lamellar substrates. This suggests, in contrast to the conclusions reached in our previous work [3], that the poly(oxyethylene) chains extending into the water layer might not interact with Laponite. It is also evident, in good agreement with our previous study [3], that both $\bar{\eta}$ and the Caillé parameter predicted by the Helfrich model are essentially independent of Laponite content in the sample.

4. Summary

A transition between a H phase formed from rod-like micelles and a L phase has been observed in a mixture of a concentrated block copolymer in water upon addition of synthetic clay, Laponite RDS. The block copolymer studied was a poly(oxyethylene)-poly(oxypropylene)-poly(oxyethylene) triblock, Pluronic P123, which is a non-ionic surfactant. This work complements prior work on the influence of added Laponite on the L and sponge phases of low molar mass nonionic surfactants [6].

The transition from H phase in a 50 wt% block copolymer solution to a L phase on addition of Laponite, at sufficiently high temperature, is tentatively ascribed to a difference in packing entropy of the disk-like particles in the two phases. There is a "packing frustration" for disks in the H phase due to a reduced excluded volume.

The form factor of the Laponite particles confirmed them to be disk-like, with a diameter $2R = 35$ nm, and thickness $\Gamma = 2$ nm. Using these dimensions, together with the density and amount of added laponite and the calculated thickness of the water layer between block copolymer lamellae, enabled the average separation between Laponite particles to be calculated in the L phase. It was thus shown that there was ample space to accommodate them within the water layer. The spacing between particles decreased with increasing Laponite content, as expected.

The structure factor in the vicinity of the Bragg peaks in the L phase was analysed using the Caillé model, from which an average Caillé exponent was determined from fits to all orders of reflection. This was found to be essentially independent of Laponite content, showing that the "stiffness" of the lamellae does not depend on the amount of added Laponite.

Acknowledgements.

We thank Prof. Wim de Jeu (AMOLF, Netherlands) for discussion concerning structure factors of smectic phases.

References

- [1] Hamley, I. W. (2000) *Introduction to Soft Matter*, John Wiley: Chichester.
- [2] Giannelis, E. P., Krishnamoorti, R., Manias, E. (1999) *Adv. Pol. Sci.*, **138**, 108.
- [3] Castelletto, V., Ansari, I. A., Hamley, I. (2003) *Macromolecules*, **36**, 1694.
- [4] Schmidt, G., Nakatani, A. I., Butler, P. D., Han, C. C. (2002) *Macromolecules*, **35**, 4725.
- [5] Grillo, I., Levitz, P., Zemb, T. (1999) *Eur. Phys. J. B*, **10**, 29.
- [6] Grillo, I., Levitz, P., Zemb, T. (2001) *Eur. Phys. J. E*, **5**, 377.

- [7] Mourchid, A., Delville, A., Lambard, J., Lecolier, E., Levitz, P. (1995) *Langmuir*, **11**, 1942.
- [8] Mourchid, A., Lecolier, E., van Damme, H., Levitz, P. (1998) *Langmuir*, **14**, 4718.
- [9] Levitz, P., Lecolier, E., Mourchid, A., Deville, A., Lyonnard, S. (2000) *Europhys. Lett.*, **49**, 672.
- [10] Knaebel, A., Bellour, M., Munch, J.-P., Viasnoff, V. (2000) *Europhys. Lett.*, **52**, 73.
- [11] Cousin, F., Cabuil, V., Levitz, P. (2002) *Langmuir*, **18**, 1466.
- [12] Holmqvist, P., Alexandridis, P., Lindman, B. (1998) *J. Phys. Chem. B*, **102**, 1149.
- [13] Wanka, G., Hoffmann, H., Ulbricht, W. (1994) *Macromolecules*, **27**, 4145.
- [14] Pople, J. A., Hamley, I. W., Fairclough, J. P. A., Ryan, A. J., Komanschek, B. U., Gleeson, A. J., Yu, G.-E., Booth, C. (1997) *Macromolecules*, **30**, 5721.
- [15] Hamley, I. W., Pople, J. A., Gleeson, A. J., Komanschek, B. U., Towns-Andrews, E. (1998) *J. Appl. Cryst.*, **31**, 881.
- [16] Guinier, A., Fournet, G. (1955) *Small angle scattering of x-rays*, Wiley: New York.
- [17] Kroon, M., Wegdam, G. H., Sprik, R. (1996) *Phys. Rev. E*, **54**, 6541.
- [18] *International Tables for X-ray Crystallography*, Kynoch Press: Birmingham, 1959, Vol. II.
- [19] Caillé, M. A. C. R. (1972) *Acad. Sci. Paris*, **274**, 891.
- [20] Safinya, C. R., Roux, D., Smith, G. S., Sinha, S. K., Dimon, P., Clark, N. A., Bellocq, A. M. (1986) *Phys. Rev. Lett.*, **57**, 2718.
- [21] Roux, D., Safinya, C. R. (1988) *J. de Phys.*, **49**, 307.
- [22] Kaganer, V. M., Ostrovskii, B. I., de Jeu, W. H. (1991) *Phys. Rev. A*, **44**, 8158.
- [23] Helfrich, W. *Zeit. Natur. A.* (1978) *Phys. Sci.*, **33**, 305.